Simulating Stroke-Impaired Reaching Using a Population Vector Model of Cortical Control

Mario Iobbi
Physics

Author

An avid fan and player of soccer, Mario Iobbi believes that life should be stimulating to both the mind and body. "Most every Friday you'll find me playing indoor soccer at the Rec Center." When not participating in the physically active side of life, Mario works toward a career in the field of biomedical engineering. According to Mario, the driving force behind his work is "the final product, which is by far the most rewarding part of research. There is a genuine satisfaction to be attained from having a tangible representation of all the hard work."

Abstract

Motor areas of the cortex have been hypothesized to control arm movement using population vector coding. In this scheme, each neuron's activity is mathematically represented as a movement direction vector. By taking the vector sum over a large distribution of cells, a population vector is generated which has been found to point in the hand's movement direction. We attempt to explain the reaching impairments stroke victims commonly experience by adapting this population vector model to include simulated cell death as well as an inherent firing rate variability. Assuming strokes destroy neurons without preference, cell death is modeled by randomly eliminating vectors. The resulting vector sum begins to skew away from the desired movement direction. Comparisons to data from stroke subjects performing center-out reaching tasks reveal similar trends in initial movement direction error as a function of stroke severity. Furthermore, the simulation suggests a quantitative relationship between a common arm assessment scale used in clinical evaluations and the fraction of neural loss.

Key Terms

- Hemiparesis
- Population Vector
- Reaching
- Stroke

Faculty Mentor

Participating in faculty-mentored undergraduate research is a great way to exercise your creativity and invent a new device, technique, or idea. For example, Mario's paper provides support for the new idea that movement deficits after stroke can be modeled by damaging an experimentally identified neural code. This idea is important because it provides insight into why it may be difficult to move the arm after stroke, and thus what neuroregeneration or neuroengineering techniques might do to restore dexterity. My advice is to follow Mario's example: develop useful skills by working hard in your classes, find an area that excites you, hook-up with a professor, and exercise your creativity through undergraduate research.

David Reinkensmeyer
Henry Samueli School of Engineering

Introduction

This year more than 500,000 Americans will suffer a stroke, and approximately 40 percent of the survivors will be left with chronic movement deficits (Parker et al., 1986; Nakayama et al., 1994; Gray et al., 1990). Although progress has been made in describing kinematic and dynamic features of stroke-impaired movement, little is known about the mechanisms by which these features arise. The purpose of this study was to test whether a population vector model of cortically controlled hand movement, damaged to simulate the consequences of stroke, can account for a common feature of stroke-impaired reaching: increased trajectory variability.

Population vector models are based on the observation that the firing rates of motor cortical cells vary with respect to the hand's movement direction during center-out reaching tasks (Georgopulos et al., 1998). Each cell has a highest mean firing rate corresponding to one preferred movement direction, which is broadly tuned across a range of directions. A neuron can be mathematically modeled as a vector pointing in the neuron's preferred direction. To form a population vector for a given movement, each cell's vector is scaled by its mean firing rate, and a linear sum is taken across all scaled vectors. As was shown first for constrained 2-D reaches and later for free reaching in 3-D space, the population vector points in the same direction as the hand's movement direction (Georgopulos et al., 1998; Scwartz et al., 1999). Such population vector coding has been found for the primary motor cortex, premotor cortex, Area V of the parietal cortex, and the cerebellum.

Stroke can cause widespread neuron destruction in each of these areas. Perhaps the most visible result of this destruction is weakness (hemiparesis). However, detailed kinematic analysis of reaching movements following stroke has also shown that directional control of reaching movements is commonly affected (Roby-Brami et al., 1997; Beer et al., 2000; Levin, 1996). In particular, the ability to steer the arm in the desired initial movement direction is impaired, and the directional variability associated with multiple reaches is increased (Takahashi and Reinkensmeyer, 2001). Recently, the firing rate variability of individual neurons was analyzed as a function of their mean firing rate. A power function was found to successfully model this variability for multiple cortical areas. We hypothesized that neural noise, incorporated into a population vector model modified to reflect widespread neural destruction, might account for the increased directional variability in reaching following stroke. To test this hypothesis, we developed a population vector model of reaching control that incorporated previously measured levels of neural noise. The model was then used to fit experimentally observed directional reaching variability in stroke subjects. The model adequately captures the dependence of directional variability on stroke severity and predicts key features of that dependence.

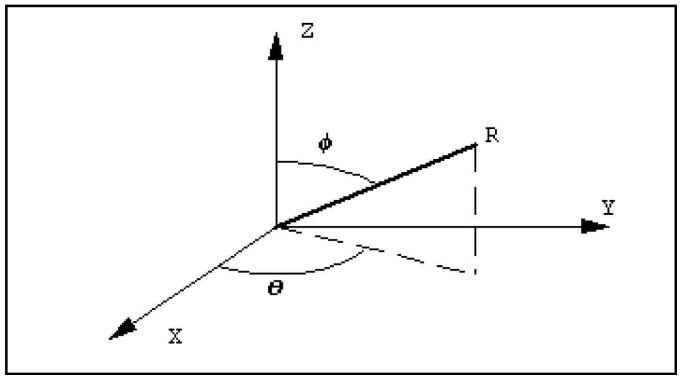

Figure 1
Reference frame for neuron modeling. Note: only population vectors are labeled by upper case Θ and Φ.

Methods

Computer Simulation

By recording individual action potentials from neurons in the motor cortex of rhesus monkeys, Georgopulos first described the phenomenon he termed "directional tuning." During center-out reaching tasks, he observed that the firing rate of each neuron varied with respect to the hand's movement direction (Georgopulos et al., 1982). In particular, each cell had a highest mean firing rate corresponding to one preferred movement direction. For movement directions other than in the preferred direction, the cell's mean firing rate was found to decrease as given by Equation 1:

$$R = b + k \cos q_p \qquad (1)$$

where b and k are fitting coefficients, R represents the neuron's mean firing rate, and θ_p is the angle between the hand's actual movement direction and the preferred movement direction. Georgopulos *et al*. modeled the neurons mathematically as vectors pointing in their preferred directions. The magnitude of the vectors was hypothesized to encode for the neurons' mean firing rates. After recording an adequate distribution of cells, these vectors can be summed together to form a population vector that points in the actual direction of hand movement. Thus Georgopulos *et al*. identified a region of the motor cortex associated with directional control of reaching.

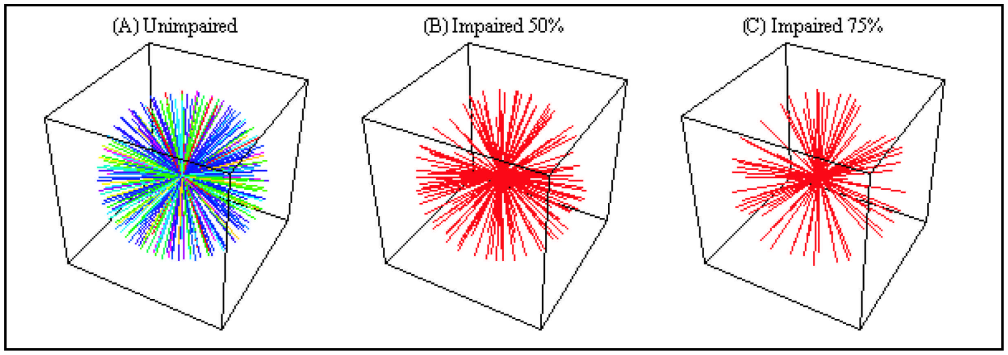

Figure 2
Vector representation of motor cortex. (A) Unimpaired virtual cortex. (B) 50% Impaired virtual cortex. (C) 75% Impaired virtual cortex.

In accordance with the population vector model, neurons of the motor cortex were modeled using several hundred-unit vectors pointing uniformly outward from a single point, as shown in Figure 2A. A healthy virtual cortex contained 322 unit vectors, a number chosen arbitrarily. Strokes were simulated by randomly eliminating a given percentage of these 322 unit vectors. Figures 2B and C show the virtual cortex with 50% and 75% of the unit vectors removed.

Strokes are localized events affecting particular areas in the brain. However, there is no current evidence supporting any topographical mapping of neurons according to their preferred movement directions. Therefore, the simulation assumed that neurons are not arranged according to preferred movement directions and cell death was approximated randomly. Using a random number generator ensured that no two strokes would be identical. Hence the surviving unit vectors described a unique virtual cortex corresponding to one particular simulated stroke subject.

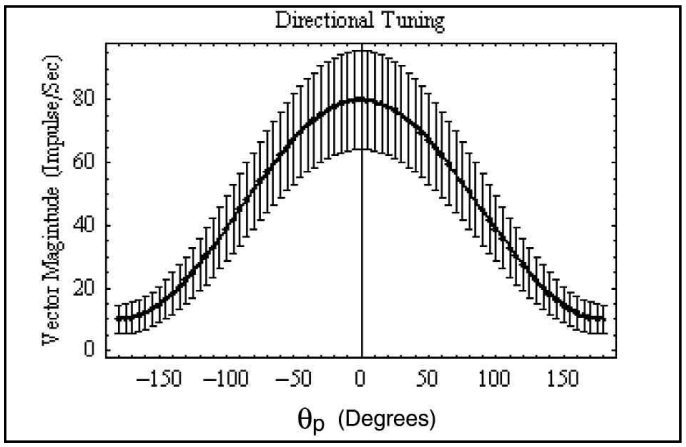

Figure 3
Mean firing rate as a function of the angle between the desired and preferred vectors.

In order for a simulated subject to reach, the virtual cortex was supplied with a desired movement direction, another unit vector. As described in Equation 1, a neuron's mean firing rate is a function of the angle between its preferred movement vector (**P**) and the desired movement vector (**D**). Equation 2 shows that the dot product of two unit vectors is equal to the cosine of the angle between them (θ_P).

$$\cos\theta_p = \vec{D} \bullet \vec{P} \qquad (2)$$

After dotting a vector from the virtual cortex against the desired vector to obtain θ_P, Equation 1 can be used to yield the mean firing rate (R) of that neuron. This mean firing rate is then set equal to the vector's magnitude. Figure 3 shows how a vector's magnitude varies as a function of θ_P.

In vivo, neurons have a high degree of variability in their mean firing rate, as depicted by the error bars in Figure 3. The equation for the standard deviation of the variability is given in Equation 3 (Takahashi and Reinkensmeyer, 2001):

$$dR = 1.2165\, R^{0.5866} \qquad (3)$$

where dR is the standard deviation in the mean firing rate. Once each surviving vector is dotted against the desired vector and given a new vector magnitude (R), they are summed together to form the population vector (Appendix). For a healthy virtual cortex, the population vector points in the same direction as the desired vector, (Figure 4A). However, simulated stroke subjects will experience an offset in their population vector with respect to the desired vector (Figure 4B).

The simulation also accounts for the standard deviation in the mean firing rate, Equation 3. Variability in the neurons' mean firing rates will inevitably create small errors in the population vector. Assuming the standard deviation in each neuron is independent from that of other neurons, the standard deviation can be calculated in the population vector direction using Equation 4.

$$\delta q = \sqrt{\left(\frac{\partial q}{\partial x_1}\delta x_1\right)^2 + \cdots + \left(\frac{\partial q}{\partial x_n}\delta x_n\right)^2} \qquad (4)$$

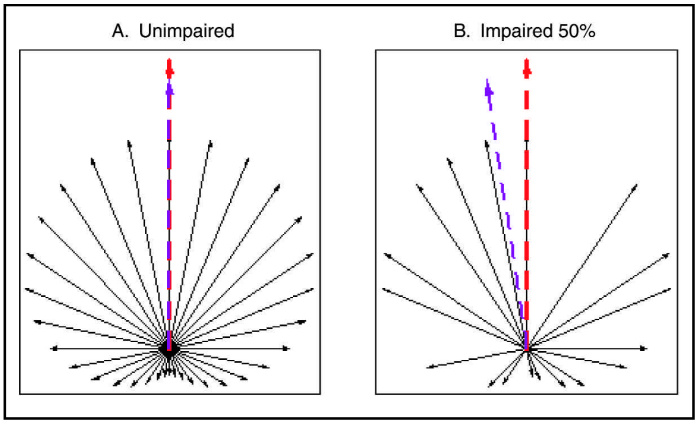

Figure 4
Active virtual cortex. Lines symbolize individual neurons. The purple arrow represents the population vector, while the red arrow represents the desired vector. (A) Unimpaired. (B) Impaired.

This general equation for independent error was used to find $\delta\Theta$, the standard deviation of Θ in the population vector (exact equation given in Appendix). Figure 5 shows the probability of being a distance Δ away from Θ. The final step of the simulation was to incorporate this normal probability distribution described by $\delta\Theta$ to create a random offset in the population vector. To evaluate the model, predictions for movement direction errors were compared with data from two experiments with stroke subjects.

Single Target Experiment

Nine chronic hemiparetic subjects, ranging in age from 34 to 76, participated in the study approved by the Institutional Review Board (IRB) of the University of California, Irvine, under protocol #99-2326 (Takahashi and Reinkensmeyer, 2001). The subjects' hands were attached to a lightweight robotic arm (PHANToM 3.0, SensAble Technologies, Inc) through a customized orthopedic splint. The robot was used to measure the hand's position in 3-D space at a sample rate of 200 Hz. Subjects were seated, and a harness was employed to restrain any torso movements. Before and between reaches, subjects were directed to rest their hands on their laps. Upon instruction, the subject raised his/her hand to a physical start target several inches above his/her lap. Then a sound signaled him/her to reach out to a physical finish target positioned directly in front (ventrally) of the subject. The finish target was aligned with the reaching shoulder, and just inside the boundary of the reaching workspace. If the subject was unable to attain the finish target within six seconds, he/she was directed back to his lap. Subjects were given a one second rest in the lap position. After each movement, a computer provided feedback on the reach time. A desired reach time was determined by taking the mean time of the first ten reaches and used to establish uniformity. Periodic breaks were given to avoid fatigue. Subjects were selected for their ability to attain the start target and consistently move closer to the finish target.

Multiple Target Experiment

Twenty subjects, 16 with hemiparetic stroke, volunteered for the study (Kamper et al.). Subjects ranged in age from 30 to 85 years, with arm impairment levels ranging from mild to severe. The subjects were asked to perform 150 reaching movements, 75 with each arm. Each reach was directed at a target chosen at random from a set of 75 evenly spaced along 5 latitudinal rows and 15 longitudinal columns separated by 12 degrees in both directions. Subjects were positioned such that their sternoclavicular notches were aligned with the middle of the target area. The subject's trunk was restrained with a Four Point Harness (Dynaform, Adaptive Engineering Lab, Inc), and their wrists were splinted to prevent wrist flexion. From an initial posture with the hand on the lap and palm resting against the body, subjects were instructed to reach at a comfortable pace to a point as close as possible to the target without displacing their trunk, maintain that position for one second, and return to the starting position. Again subjects were allotted periodic breaks to minimize fatigue. A Flock of Birds sensor (Ascension Technology Corporation) was attached to the hand to measure its position and orientation. Hand config-

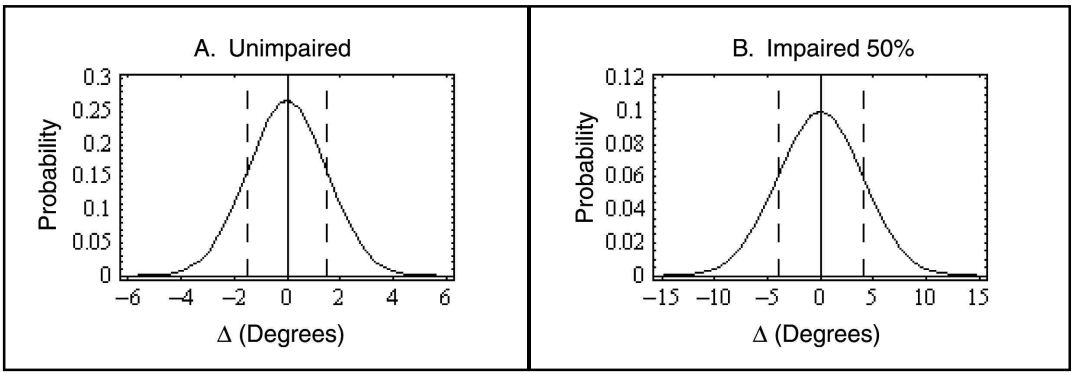

Figure 5
Probability plots of the population vector being an offset Δ away from Θ, set at zero degrees. The dashed lines represent $\pm\ \delta\Theta$. (A) Typical values for unimpaired reaching. (B) Typical values for 50% impaired reaching.

uration data was gathered at a sampling rate of 100 hz. The large number of columns compared to rows made analysis of the initial Θ movement direction more statistically useful. Correspondingly, all data and analysis was limited to the study of this one angle. (Note: Θ refers to population vectors or hand movement direction. Lower case θ refers to individual neuron directions.)

Model and Data Analysis

For both the experiments and simulations, the positive x-axis was defined as pointing directly outward in front of the seated subject (Figure 1). Movement angles sweeping toward the subject's left were declared positive and right movement angles were negative. For both clinical trials, initial movement directions were obtained from the hand trajectory data by using a 5 cm cutoff. The initial movement direction was the direction of the vector described by the start position and the point along the hand trajectory a distance 5 cm away from the start position. Data from the impaired arm were referenced against data from the unimpaired arm. Using the symmetry of the experimental setup about the xz plane, data from the unimpaired arm served as the desired direction for the impaired arm by inverting the sign of the initial movement direction.

In the computer simulation, virtual subjects were designed to follow the same protocol as their actual counterparts. If stroke subjects reached twenty times to a single target, virtual subjects also executed twenty reaches. The performance of the virtual subjects was assessed by the deviation between their desired movement direction and the direction of their population vector. Similarly, the performance of stroke subjects was assessed by the deviation between their desired direction and the initial movement direction of their impaired arm.

Prior to the trials, experienced therapists diagnosed the stroke subjects with a Chedoke-McMaster Stroke Arm Assessment score to rate their level of impairment. These scores serve as an evaluation tool that has been shown to have high inter- and intra-rater repeatability, as well as strong correlation with the Fugl-Meyer score (Kamper et al.; Lee et al., 1998; Gowland et al., 1995). Low Chedoke scores such as 2 or 3 indicate severe arm impairment while a score of 7 would indicate an unimpaired subject. A similar diagnostic scale, called stroke severity, was developed for the virtual stroke subjects, in which the scores were obtained by subtracting their damage fraction from unity.

A single measurement was developed to yield a numerical value by which to measure the net amount of initial movement direction error each subject demonstrated. This measurement was the root mean squared error (RMS) and was used to evaluate data from both clinical trials. Subjects with a large amount of deviation between their desired directions and initial movement directions received a larger RMS value than those with small deviations. For the single target stroke data, the desired direction was taken from the average over a subject's twenty unimpaired arm reaches. Meanwhile, data from the multiple target task were analyzed using a single reach to the corresponding target as the desired direction. The same RMS measurements were also made for virtual subjects.

Results

Single Target Data

Figure 6 shows some typical subjects' histograms for twenty reaches to a single target. The left column displays data from stroke subjects and the right column contains data from virtual subjects. All subjects are organized top to bottom as least impaired to most severely impaired. The histograms' horizontal axes represent the deviation angle between a reach by a subject's impaired arm and the mean desired direction as measured from their unimpaired arm.

Unimpaired subjects exhibited no significant mean deviation from the mean desired direction. Furthermore, their reaches showed only some small variation about the mean desired direction. In contrast, the impaired subjects exhibited a significant mean deviation from the mean desired direction. Additionally, their reaches also exhibit increased variability as compared to unimpaired subjects. The same trends were present in the stroke subjects as well as the virtual subjects.

Multiple Target Data

Figure 7 shows typical plots of subject data for the multiple target-reaching task. Each point on the plot is defined by two reaches. The initial movement direction from a subject's unimpaired arm to a particular target is the desired direction. The initial movement direction of the impaired arm to the corresponding target defines the impaired direction. Data points for unimpaired subjects lie roughly along the diagonal line because there was little deviation between the initial movement direction of one arm compared with the other arm. However, subjects with increasing impairment display a pronounced deviation from the diagonal. This trend is indicative of the initial movement direction errors commonly associated with patients after strokes. A similar characteristic deviation from the diagonal was shown by the reaching data of the virtual subjects.

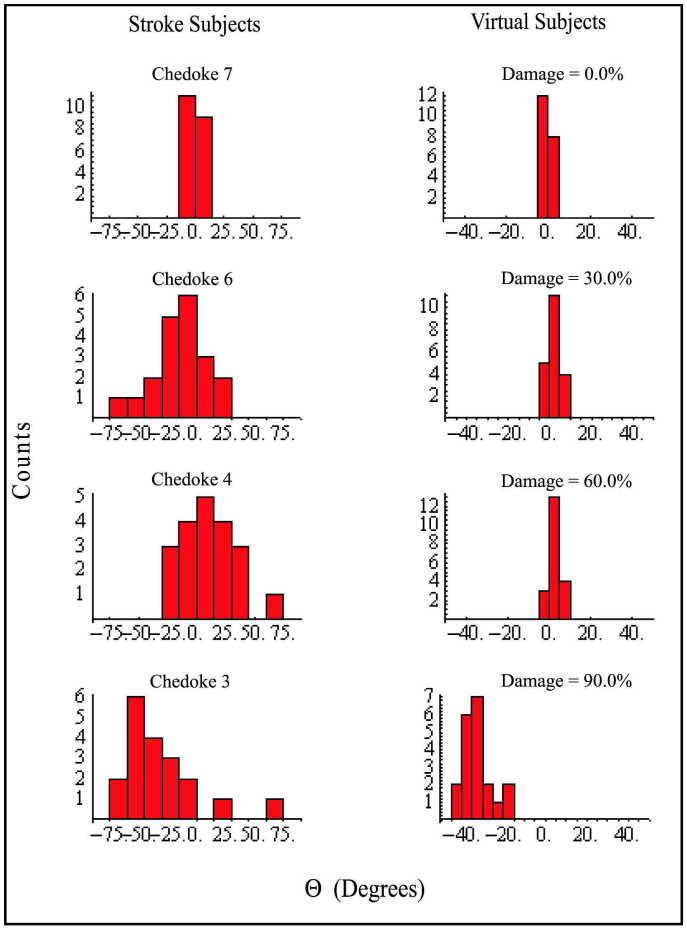

Figure 6
Histograms of single target clinical trial. The mean desired direction is set equal to zero degrees in all cases.

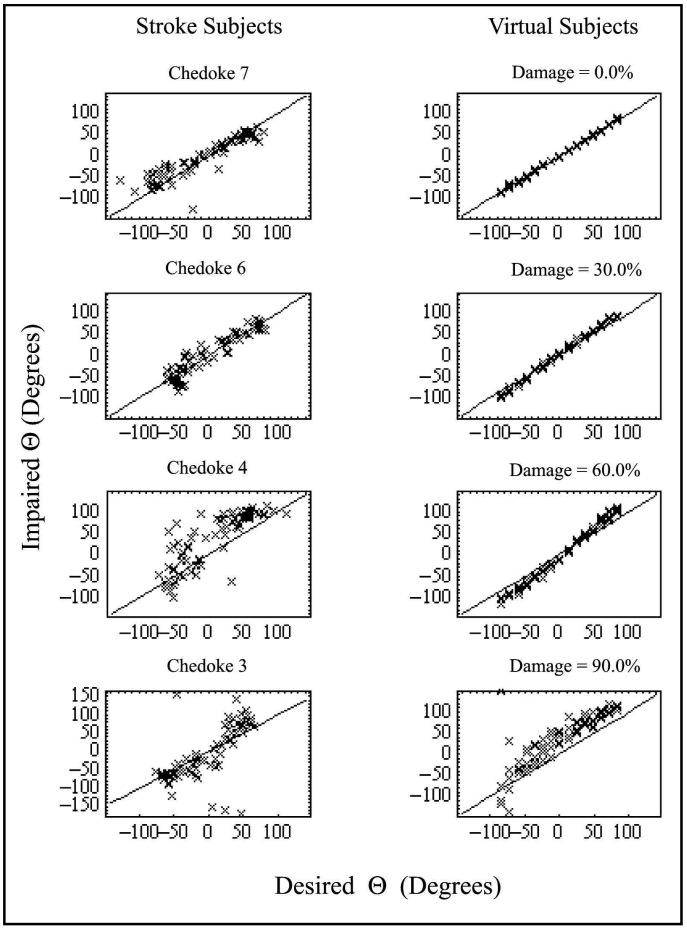

Figure 7
Plots of desired directions versus impaired arm initial movement directions.

RMS Data

All the results are shown in Figures 8 and 9. In general, stroke subjects diagnosed as having one particular Chedoke score did not have a single RMS value, but rather exhibited a range of RMS values. For example, the stroke subjects diagnosed as Chedoke 3 during the single target trial ranged in RMS values from 17 to 38. Only in the case of unimpaired subjects does the RMS range converge close to a single point. In fact, the RMS range appeared to be related to the level of stroke impairment. Figure 9A shows how stroke subjects with higher levels of impairments demonstrated a much wider range of RMS values than unimpaired subjects. This Chedoke-dependent spreading also appeared in the stroke subject data for the single target task in Figure 8A. All data sets were fit using a three-parameter exponential decay given in Equation 5, and used for subsequent analysis.

$$RMS(x) = A + Be^{-x/C} \qquad (5)$$

The population vector model data closely approximated the observed data. The stroke severity-dependent spreading is even more pronounced in the simulation due to the greater number of virtual subjects. Unimpaired subjects received approximately a single RMS value, while the most impaired subjects varied in their RMS values. However, the simulation consistently predicted lower RMS values for all subjects from the most severely impaired to the unimpaired in both trials. Stroke subjects with a Chedoke score of 7 during the multiple target task received a mean RMS value of around 20 degrees while their virtual counterparts only scored about 2. Unimpaired subject RMS scores from the single target task shown in Figure 8 likewise have similar values. The simulator systematically underestimates the total amount of reaching variability.

The simulation was designed to account for a particular amount of variation attributable to the noisy nature of a neuron's mean firing rate. Nevertheless, the stroke subjects,

particularly the unaffected subjects, displayed a far greater amount of variability than could be accounted for by their virtual counterparts. *In vivo*, there are several additional sources of noise downstream of the motor cortex. The signal must filter down the nervous system to activate the muscles, and all could introduce the increased variability to the system. The simulator does not account for any downstream noise and therefore generates much smaller RMS values. We were able to reincorporate the downstream noise using one assumption. In unimpaired individuals, the discrepancy between the predicted RMS value and the measured RMS values is attributed to downstream noise. This assumption is incorporated into Equation 6.

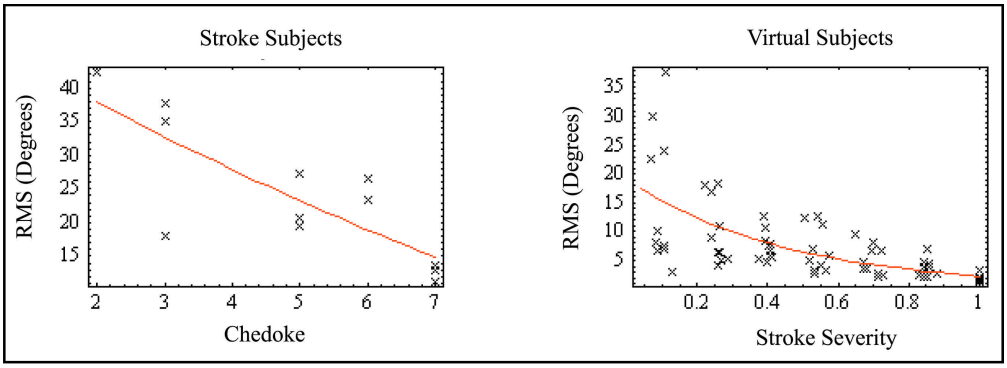

Figure 8
Single target RMS versus impairment level. Note: The red line represents a best fit curve.

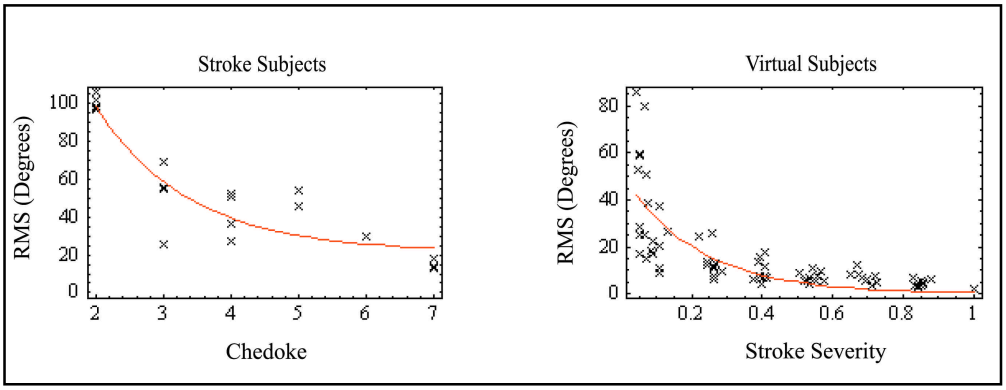

Figure 9
Multiple target RMS versus impairment level. Note: The red line represents a best-fit curve.

$$RMS(Chedoke) = RMS(Stroke\ Severity) + K_{RMS} \qquad (6)$$

K_{RMS} is the amount of downstream noise as established by the difference between unimpaired stroke subject and virtual subject RMS values. From Equation 6, one can determine Chedoke as a function of Stroke Severity for each trial. Figure 10 depicts the two curves (red - Single Target Trial, blue - Multiple Target Trial). The overlap between the two curves suggests that the adapted population vector model adequately captures the relationship between stroke severity and directional error. In particular, using two different sets of stroke subjects with two different protocols, the model predicted similar relationships between stroke severity and Chedoke score.

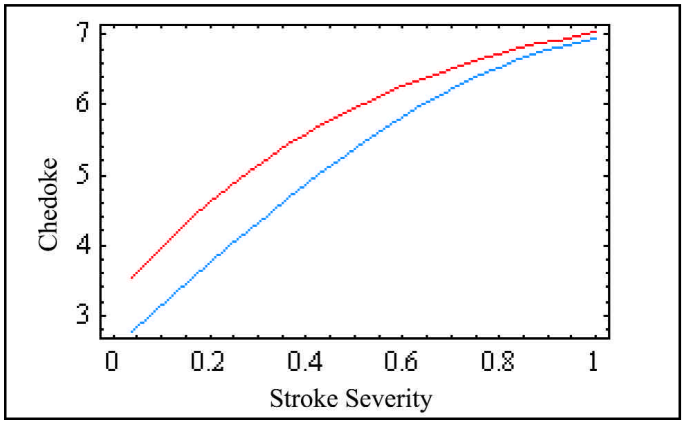

Figure 10
Chedoke vs. Stroke Severity; red: single target regression, blue: multiple target regression.

Discussion and Conclusion

Neural network models such as the population vector model have provided insight to how the brain controls high level parameters, such as the hand trajectory, through the interaction of individual neurons. The present results demonstrate that by incorporating random cell death to simulate strokes, the population vector model predicts clinically observed patterns of reaching impairment.

In this instance, the characteristic initial movement direction errors commonly exhibited by stroke patients are shown as likely having their roots in damage to one particular region of the motor cortex. The computer simulations accounts for trends in both magnitude and variation of these initial movement direction errors as a function of the stroke severity. Perhaps most important, data obtained

from the computer simulations were useful in establishing a possible link between the Chedoke clinical evaluation and the fraction of cell death experienced in the motor cortex.

As more research is conducted using the population vector, new and more powerful models are being developed (Amirikian and Georgopulos, 2000). This adaptation of the population vector uses the fundamental and most widely accepted directional tuning equation (Equation 1). New evidence suggests the population vector codes for more than just hand direction. Some researchers believe the magnitude of the population vector is a representation of the hand velocity (Georgopulos et al., 1982). Experiments on these more controversial models would yield more empirically measurable parameters and lead to more conclusive results. Understanding the operating structure of cortical networks is essential to diagnosing the obstructions impairing natural function following cerebral traumas. Ultimately, knowledge acquired from such studies will serve to better direct patient recovery and rehabilitation.

Appendix

Given a uniformly distributed spherical virtual cortex, and any arbitrarily desired direction vector, Equations 1 and 2 can be combined to yield the magnitude of every vector in that cortex. Directional tuning (Equation 1) implies each vector magnitude is a function of the angle between the desired direction and the vector's preferred direction. Equation 2 then solves for the angle between these two vectors. The net activity of the entire cortex is calculated in a vector sum using the equations given below.

$$\overline{X} = \sum_{i=1}^{N} R_i \cos(\theta_i) \sin(\phi_i) \qquad \text{(A1)}$$

$$\overline{Y} = \sum_{i=1}^{N} R_i \sin(\theta_i) \sin(\phi_i) \qquad \text{(A2)}$$

$$\overline{Z} = \sum_{i=1}^{N} R_i \cos(\phi_i) \qquad \text{(A3)}$$

X, Y, Z are the Cartesian sum of the N total vector components. They can be translated back into polar coordinates using Equations A-4 and A-5. Only the Θ direction was useful for data analysis .

$$\Theta = \arctan\left(\frac{\overline{Y}}{\overline{X}}\right) \qquad \text{(A4)}$$

$$\Phi = \arctan\left(\frac{\sqrt{\overline{X}^2 + \overline{Y}^2}}{\overline{Z}}\right) \qquad \text{(A5)}$$

The Θ direction can be directly compared to the desired θ for any deviation. Variation in the Θ was calculated using Equation A-4 as well as combining Equation 3 and substituting it in Equation 4 from the text. The final solution is given below (Equation 6):

$$\delta\Theta = \sqrt{\sum_{j=1}^{N} \frac{[\overline{X}\sin(\theta_j)\sin(\phi_j) - \overline{Y}\cos(\theta_j)\sin(\phi_j)]^2}{[\overline{X}^2 + \overline{Y}^2]^2} (\delta R_j)^2}$$

Acknowledgments

I would like to thank Dr. Reinkensmeyer for his excellent mentorship. This project was supported by an Undergraduate Research Opportunities Program Grant.

Works Cited

Amirikian, B., A.P. Georgopulos. "Directional Tuning Profiles of Motor Cortical Cells." Neuroscience Research 36 (2000): 73-79.

Beer, R.F., J.P.A. Dewald, and W.Z. Rymer. "Defects in the Coordination of Multijoint Arm Movements in Patients with Hemiparesis: Evidence for Disturbed Control of Limb Dynamics." Experimental Brain Research 131 (2000): 305-319.

Fugl-Meyer, A.R., L. Jaasco, L. Leyman, S. Olsson, and S. Steglind. "The Post-Stroke Hemiplegic Patient." Scandinavian Journal of Rehabilitation Medicine. 7 (1975): 13-31.

Georgopoulos, A.P., J.F. Kalaska, R. Caminiti, and J.T. Massey. "On the Relations Between the Direction of Two-Dimensional Arm Movements and the Cell Discharge in the Primate Motor Cortex." Journal of Neuroscience 2 (1982): 1527-1537.

Georgopoulos, A.P., R.E. Kettner, and A.B. Scwartz. "Primate Motor Cortex and Free Arm Movements to Visual Targets in Three-Dimensional Space. Relations Between Single Cell Discharge Rates and Direction of Movement." Journal of Neuroscience 18 (1998): 1161-1170.

Gowland, C., P. Stratford, M. Ward, J. Moreland, W. Torresin, S. Van Hullenaar, J. Sanford, S. Barrecca, B. Vanspall, and N. Plews. "Measuring Physical Impairment and Disability with the Chedoke-McMaster Stroke Assessment." Stroke 24 (1993): 58-63.

Gowland, C., S. VanHullenaar, W. Torresin, J. Moreland, B.Vanspall, S. Barrecca, M. Ward, M. Huijbregts, P. Stratford, and R. Barclay-Goddard. Chedoke-McMaster Stroke Assessment: Development, Validation and Administration Manual. Hamilton, Canada: Chedoke-McMaster Hospitals and McMaster University, 1995.

Gray, C.S., J.M. French, D. Bates, N.E.F. Cartlidge, O.F.W. James, and G. Venables. "Motor Recovery Following Acute Stroke." Age and Aging 19 (1990): 179-184.

Kamper, D.G., A.N. McKenna-Cole, L.E. Kahn, and D. Reinkensmeyer. "Alterations in Reaching after Stroke and Their Relationship to Movement Direction and Impairment Severity." Archives of Physical Medicine and Rehabilitation (2002), in press.

Lee, D., N.L. Port, W. Kruse, and A.P. Georgopulos. "Variability and Correlated Noise in the Discharge of Neurons in the Motor and Parietal Areas of the Primate Cortex." Journal of Neuroscience 18 (1998): 1161-1170.

Levin, M.F. "Interjoint Coordination During Pointing Movements is Disrupted in Spastic Hemiparesis." Brain 119 (1996): 281-293.

Nakayama, H., H.S. Jorgensen, H.O. Raaschou, and T.S. Olsen. "Recovery of Upper Extremity Function in Stroke Patients: The Copenhagen Stroke Study." Archives of Physical Medicine and Rehabilitation 75 (1994): 394-398.

Parker, V.M., D.T. Wade, and R. Hewer Langton. "Loss of Arm Function after Stroke: Measurement, Frequency, and Recovery." International Rehabilitation Medicine 8 (1986): 69-73.

Research and Graduate Studies: Human Subjects Research, the University of California, Irvine. http://www.rgs.uci.edu/hs/hsindex.htm

Roby-Brami, A., S. Fuschs, M. Mokhtari, and B. Brussel. "Reaching and Grasping Strategies in Hemiparetic Patients." Motor Control 1 (1997): 72-91.

Scheidt, R.A., D. Reinkensmeyer, M. Conditt, W. Rymer, and F. Mussa-Ivaldi. "Persistence of Motor Adaptation During Constrained Multi-Joint Arm Movements." Journal of Neurophysiology 84 (2000): 853-862.

Scwartz, A.B., and D. Moran. "Motor Cortical Representation of Speed and Direction During Reaching." Journal of Neurophysiology 82 (1999): 2676-2692.

Takahashi, C.D., and D. Reinkensmeyer. "Impaired Motor Adaptation and Directional Weakness during Reaching Following Hemiparetic Stroke." Society for Neuroscience Abstracts 14 (2001): 832.